Correspondence

Dissociation of forward and convergent remapping in primate visual cortex

Sujaya Neupane*, Daniel Guitton, and Christopher C. Pack

A fundamental concept in neuroscience is the receptive field, the area of space over which a neuron gathers information. Until about 25 years ago, visual receptive fields were thought to be determined entirely by the pattern of retinal inputs, so it was quite surprising to find neurons in primate cortex with receptive fields that changed position every time a saccade was executed [1]. Although this discovery has figured prominently into theories of visual perception, there is still much debate about the nature of the phenomenon: Some studies report *forward remapping* [1–3], in which receptive fields shift to their postsaccadic locations, and others report *convergent remapping*, in which receptive fields shift toward the saccade target [4]. These two possibilities can be difficult to distinguish, particularly when the two types of remapping lead to receptive field shifts in similar directions [5], as was the case in virtually all previous experiments. Here we report new data from neurons in primate cortical area V4, where both types of remapping have previously been reported [3,6]. Using an experimental configuration in which forward and convergent remapping would lead to receptive field shifts in opposite directions, we show that forward remapping is the dominant type of receptive field shift in V4.

Figure 1A depicts a conventional remapping experiment. The subject is cued to execute a saccade, in a direction indicated by the black arrow. The receptive field of a single neuron (blue circle) is located just below the fixation point, so that forward remapping would cause it to shift leftward and downward (green arrow and circle). On the other hand, convergent remapping would cause it to shift leftward and slightly upward (grey arrow and circle). The distinction between the two remapping directions is subtle, particularly relative to the coarse sampling of space used in most previous studies [1]. As a result, the interpretation of this kind of data has been controversial, with different groups arriving at different conclusions, even when recording from the same brain regions [3,6–8]. Recent evidence for forward remapping comes from a study in which saccades were made in a direction opposite the visual receptive fields [3]. However, even in this case the two remapping directions were similar (Figure 1A), and at least one computational model has claimed to accommodate this type of result under the assumption that remapping is exclusively convergent [5].

The decisive experiment is depicted in Figure 1B. Here the saccade target is positioned so that forward and convergent remapping would yield nearly opposite results: Forward remapping would entail a shift away from the saccade target [1], while models of convergent remapping predict a shift toward the saccade
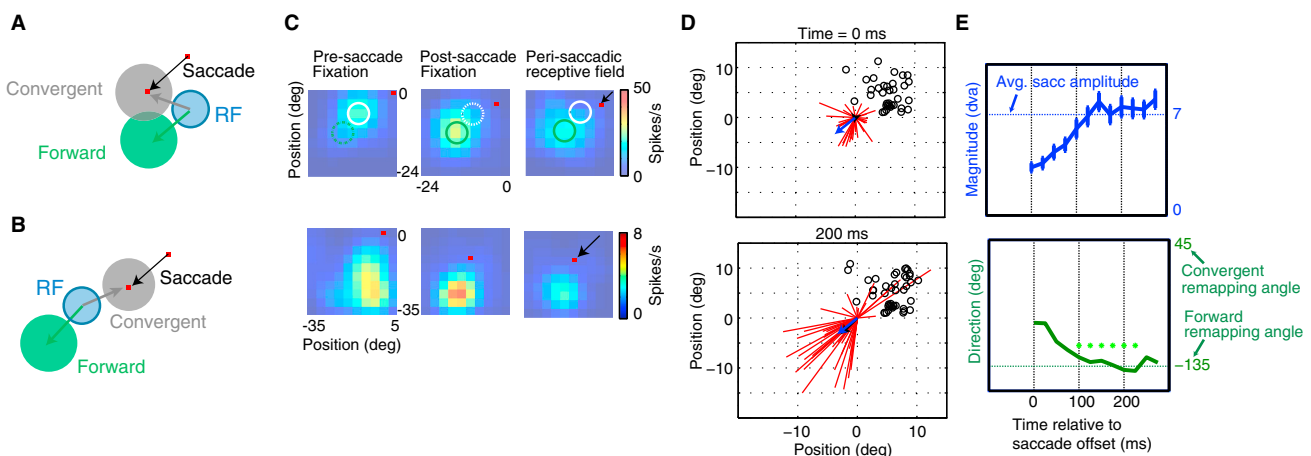

Figure 1. Geometry of forward and convergent remapping.
Forward remapping (green) is a shift of the receptive field (blue) according to the saccade vector (black). Convergent remapping (grey) is a shift of all receptive fields toward the saccade target (red). Most experiments have an arrangement similar to (A), wherein the two types of remapping overlap. By contrast, the experimental configuration in (B) permits a complete dissociation of forward and convergent remapping. (C) Example V4 neurons in which the receptive field was mapped before (left) and after (middle) a downward-leftward saccade. For the neuron in the top row, the saccade length was 6°, and for the one in the bottom row it was 14°. For stimuli flashed just before the saccade (right), the receptive fields evaluated at 200 ms after the saccade resembled the post-saccadic receptive field, consistent with forward remapping. (D) Remapping in the V4 population. The origin of each plot represents the center of each fixation receptive field. Black circles show the direction of convergent remapping, while the blue arrow represents the direction of forward remapping. Each red line represents the observed remapping shift for one V4 neuron. (E) Time-course of remapping. The blue line (top) shows the average length of remapping vectors for the V4 population across time. The green line (bottom) shows the mean remapping vector angle. Data are represented as mean ± SEM. Green asterisks indicate time points at which the population remapping vector was significantly tuned (Rayleigh test, p < 0.001).

target [5]. We exploited this geometry to dissociate the two types of remapping, using an approach that has been described previously [3] (see Figure S1 in the Supplemental Information).

Figure 1C (left) shows the receptive fields of two example V4 neurons during fixation (left), before the execution of a 6° (top) or 14° (bottom) down-leftward saccade. During fixation at the postsaccadic eye position (middle), the receptive fields remained stable in retinal coordinates, in approximately the same locations relative to the fixation point. Crucially, for stimuli flashed just before saccade onset, the receptive fields shifted *away* from the saccade target (right panel), toward the postsaccadic locations, as expected for forward remapping (additional examples are shown in Figure S2).

Figure 1D summarizes our results for a population of 53 V4 neurons, chosen so that the shifts associated with forward and convergent remapping were separated by at least 110° (range: 113–179°, mean 165°). Each red line represents the observed perisaccadic shift of one neuron's receptive field, and the distribution of these *remapping vectors* indicates the pattern of remapping across the population. The open circles show the convergent remapping directions, while the blue arrow shows the forward remapping direction.

Early in the post-saccadic period (Figure 1D, top), there was no consistent direction of remapping (Rayleigh non-uniformity test, p > 0.05), but 200 ms later there was robust, forward remapping (Figure 1D, bottom); few neurons showed convergent remapping (one is shown in Supplemental Figure S2B). For the population, the mean remapping vector angle was -139°, which was not significantly different from that of the saccade (Watson-Williamson two-sample test; $F_{1,104} = 0.031$, p = 0.860). The strength of tuning for the population vector was significantly different from a random distribution (Rayleigh non-uniformity test, p < 0.001) and from a shuffled version of the actual data (two-sample t-test, p < 0.001). Figure 1E shows the time course of the mean remapping vector, which evolved toward the forward

remapping direction (bottom) and magnitude (top) after the saccade. There is little evidence for convergent remapping at any time point, presumably because such responses are outweighed by those in the forward remapping direction [3].

These results demonstrate unambiguously that forward remapping occurs in area V4, and in fact that such responses are both more common and higher in amplitude than those associated with convergent remapping. This result appears to be incompatible with models that rely exclusively on convergent mechanisms, centered on the saccade target, to generate remapping [5]. At the same time, we do not dispute that convergent remapping can result from covert and overt attentional shifts [3,5,8,9], independently of forward remapping [1]. The relative strengths of the two types of remapping likely depend on the experimental configuration and the recording site.

More generally, these results and others [1,8] highlight the complexity of spatial representations in the primate brain. An emerging pattern of results shows that the perisaccadic responses of V4 neurons recall the locations of past stimuli [3] and anticipate potential future stimuli [6,10], in addition to their well-known roles in shape recognition and attention. The fact that these different responses are present in the same area, and often in the same neurons, has profound implications for theories of spatial representations in the primate brain [2,4].

SUPPLEMENTAL INFORMATION

Supplemental Information includes a detailed description of the experimental paradigms and analyses, as well as additional example neurons, and can be found with this article online at http://dx.doi.org/10.1016/j.cub.2016.04.050.

ACKNOWLEDGEMENTS

REFERENCES

1. Duhamel, J.R., Colby, C.L., and Goldberg, M.E. (1992). The updating of the representation of visual space in parietal cortex by intended eye movements. Science *255*, 90–92.
2. Marino, A.C., and Mazer, J.A. (2016). Perisaccadic updating of visual representations and attentional states: linking behavior and neurophysiology. Front. Sys. Neurosci. *10*, 3.
3. Neupane, S., Guitton, D., and Pack, C.C. (2016). Two distinct types of remapping in primate cortical area V4. Nat. Commun. *7*, 10402.
4. Zirnsak, M., and Moore, T. (2014). Saccades and shifting receptive fields: anticipating consequences or selecting targets? Trends Cogn. Sci. *18*, 621–628.
5. Zirnsak, M., Lappe, M., and Hamker, F.H. (2010). The spatial distribution of receptive field changes in a model of peri-saccadic perception: predictive remapping and shifts towards the saccade target. Vision Res. *50*, 1328–1337.
6. Tolias, A.S., Moore, T., Smirnakis, S.M., Tehovnik, E.J., Siapas, A.G., and Schiller, P.H. (2001). Eye movements modulate visual receptive fields of V4 neurons. Neuron *29*, 757–767.
7. Sommer, M.A., and Wurtz, R.H. (2006). Influence of the thalamus on spatial visual processing in frontal cortex. Nature *444*, 374–377.
8. Zirnsak, M., Steinmetz, N.A., Noudoost, B., Xu, K.Z., and Moore, T. (2014). Visual space is compressed in prefrontal cortex before eye movements. Nature *507*, 504–507.
9. Connor, C.E., Gallant, J.L., Preddie, D.C., and Van Essen, D.C. (1996). Responses in area V4 depend on the spatial relationship between stimulus and attention. J. Neurophysiol. *75*, 1306–1308.
10. Zanos, T.P., Mineault, P.J., Nasiotis, K.T., Guitton, D., and Pack, C.C. (2015). A sensorimotor role for traveling waves in primate visual cortex. Neuron *85*, 615–627.

Montreal Neurological Institute, McGill University, 3801 University Street, Montreal, Quebec, Canada.
*E-mail: sujaya.neupane@mail.mcgill.ca

The editors of Current Biology welcome correspondence on any article in the journal, but reserve the right to reduce the length of any letter to be published. All Correspondence containing data or scientific argument will be refereed. Queries about articles for consideration in this format should be sent by e-mail to cbiol@current-biology.com

Supplemental Information: Dissociation of forward and convergent remapping in primate visual cortex

Sujaya Neupane, Daniel Guitton, Christopher C. Pack
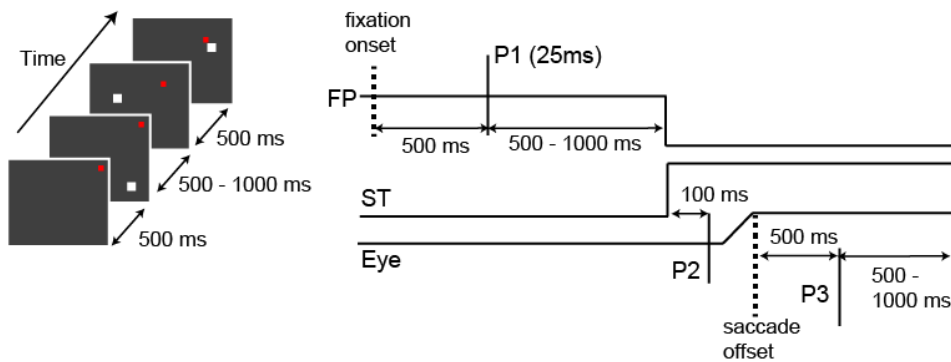
Supplemental Figures

A
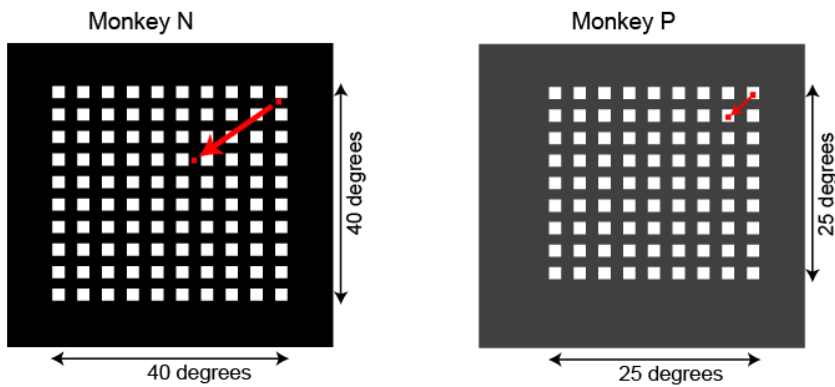
B

Figure S1. (A) Experimental design showing all potential probe locations (white squares) and the saccade vector (red arrow) for two monkeys. (B) Timing of events on each trial, starting with fixation and the first (P1) probe, followed by the appearance of the saccade target (ST) and the second probe (P2), the execution of the saccade and the presentation of the third (P3) probe.
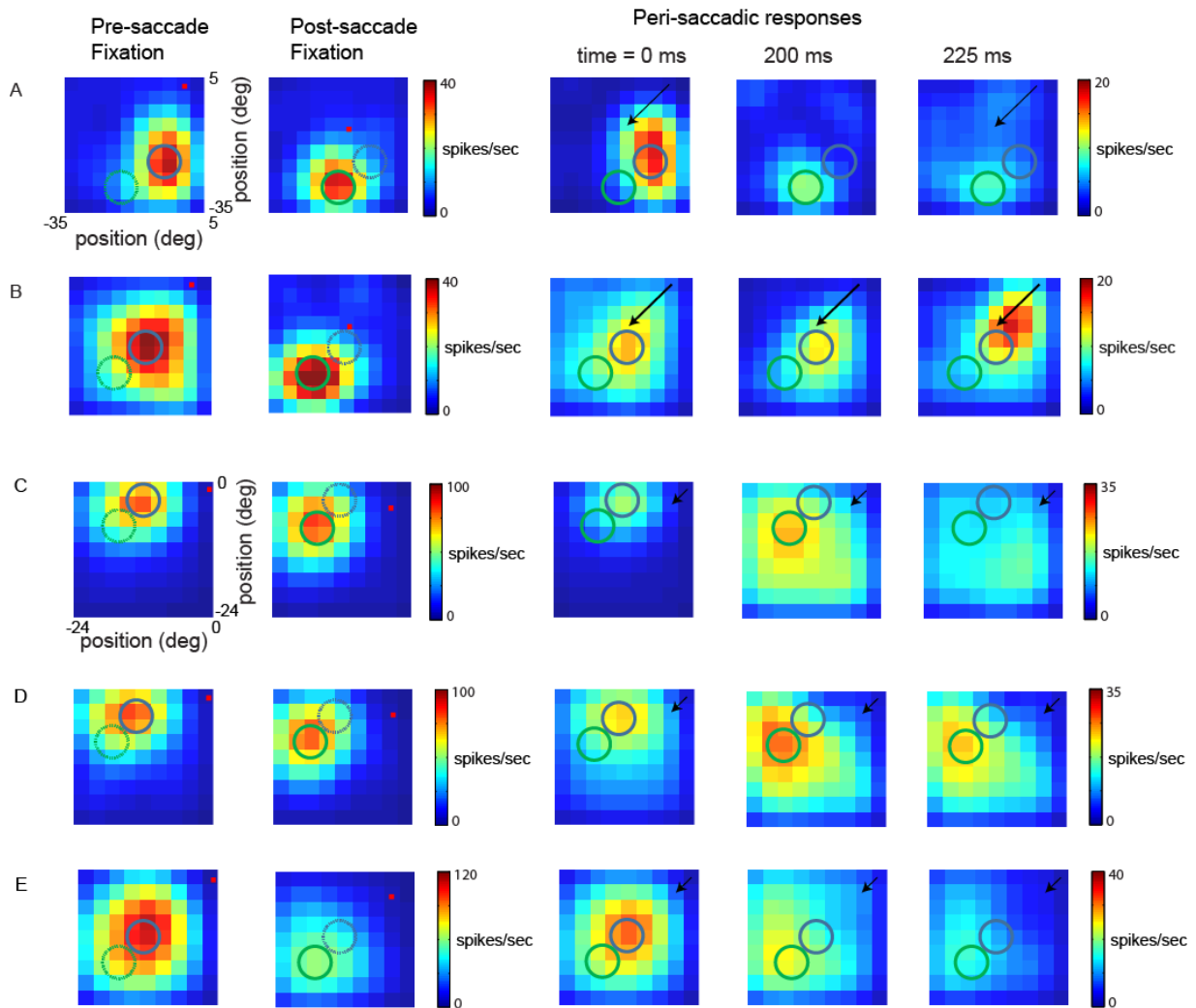
Figure S2. (A-F) Each row represents a different V4 neuron. The columns show the responses during fixation at the presaccadic location (left column) and the post-saccadic location (second from left), followed by the responses to presaccadic (P2) probes at various time points after the saccade (three rightmost columns). Strong responses are indicated by reddish colors and weak responses by bluish colors. Blue circles represent pre-saccadic receptive field location and green circles represent post-saccadic receptive field location. Receptive field maps have been smoothed for display purposes.

Supplemental Experimental Procedures

Experimental methods were identical to those describe previously [S1], with the exception of the direction and amplitude of the saccades, as described below. Here we provide a brief summary of these methods.

Electrophysiological recordings. Recordings were obtained via chronically implanted 10×10 microelectrode arrays (Utah array; Blackrock Microsystems) in area V4 of two monkeys (*Macaca fascicularis*). All aspects of the experiments were approved by the Animal Care Committee of the Montreal Neurological Institute and were conducted in compliance with regulations established by the Canadian Council of Animal Care.

From each electrode, wideband signals were recorded using a standard data acquisition system (Plexon Multichannel Acquisition Processor System), which was custom modified to facilitate separation of spikes from field potentials, as described previously [S2]. Spikes were sorted offline for each recording by first band-pass filtering the raw signal between 500 and 4000 Hz and then using an automated spike-detection algorithm [S3].

Experimental paradigm. Visual stimuli were back-projected on a semi-transparent screen by a cathode ray tube video projector, with a refresh rate of 75 Hz. The screen covered an area of $80 \times 50°$ of visual angle at a viewing distance of 78 cm. To probe receptive fields, we used white squares (luminance=22.5 cd m^{-2}) presented for 25 ms on a dark background (luminance <0.01 cd m^{-2}). Each probe was square in shape, 2° in width.

Each trial started with the animal fixating a red dot 0.5° in diameter for 500 ms, after which a visual probe (P1) was flashed at a position chosen randomly from a square grid of possible locations (Supplemental Figure 1A). The size and location of the grid were chosen to span the receptive fields of all neurons recorded simultaneously. Because the eccentricities covered by the arrays in the two monkeys were somewhat different, we adjusted the probe grids and saccade vectors accordingly: In monkey N we used 100 possible locations arranged in a 10×10 grid (4° spacing between positions), and in Monkey P, we used a 9 x 9 grid with 3° spacing between positions (Supplemental Figure 1a).

After a variable delay of 500–1,000 ms, the fixation point jumped to a new target, cuing a downward-leftward saccade at an angle of -135°; for Monkey P the saccade amplitude was 5.7°, while for Monkey N it was 14.1°. A second probe (P2) was then flashed 100 ms later, at a randomly chosen location. To ensure that P2 flashes were completely off, we measured the luminance decay on the projector screen with a photodiode. Luminance had decreased by 99% 6 ms after the probe offset; any trial in which the saccade started <40 ms after the probe offset was discarded.

Monkeys were required to make a visually guided saccade to the target and fixate there for another 500 ms, after which a third probe (P3) was flashed again at a randomly chosen location. Animals then fixated for another variable period of 500–1,000 ms, after which a liquid reward was delivered. We included data from sessions in which at least 10 trials per probe location were obtained.

Eye movements. Eye position was monitored at 1,000 Hz using an infrared eye tracker (Eyelink; SR Research). Saccade onset was defined as the time at which the eye left the 2.5° fixation window and crossed a velocity threshold of 200° s^{-1}. Saccade offset was the time when the eye

velocity dropped below 200° s^{-1}. Eye movements were processed offline to eliminate trials that contained blinks or catch-up saccades.

Data analysis. We analyzed data from 53 neurons that had receptive fields positioned in such a way that the predictions of forward and convergent remapping were separated by at least 110 deg. For each neuron, the firing rate was estimated in 25 ms time bins, at various times relative to the offset of the saccade.

We included all neurons that showed significant post-saccadic responses (one sample t-test, p<.05), relative to the pre-saccadic baseline, to at least one probe. This criterion excluded neurons that showed strong post-saccadic suppression, which occurs frequently for saccades into the same visual hemifield as the receptive fields [S1]. We deliberately used a lax inclusion criterion to avoid making any assumptions about the spatial or temporal structure of post-saccadic visual responses; as a result, many of the individual neurons showed rather noisy remapping responses (Figure 1D).

The center of each receptive field was estimated as the center of mass of activity over the probe grid at each time point [S4]. After smoothing and interpolation [S1], each probe location was weighted by its corresponding firing rate. The weighted probe locations were summed and divided by the total firing rate to obtain the receptive field center:

$$Xloc = \frac{1}{S}\sum_x \sum_y r_{xy}x$$

$$Yloc = \frac{1}{S}\sum_x \sum_y r_{xy}y$$

$$S = \sum_x \sum_y r_{xy}.$$

We used the receptive field centers to generate predictions for forward and convergent remapping (Figure 1). Forward remapping entails a shift of the receptive field center from its presaccadic to its postsaccadic locations. Convergent remapping entails a shift in the direction of the saccade target (Figure 1). The observed shifts were characterized as a remapping vector connecting the P1 receptive field center and the P2 receptive field center [S1].

We computed this remapping vector for each neuron at various time points relative to the offset of each saccade. For each time point, from the ensemble of the remapping vectors, we generated a mean population vector, the length and angle of which are plotted in Figure 1E. The predictions of forward and convergent remapping were obtained by averaging the predicted remapping vectors across data from both monkeys, and hence across both saccade lengths. This yielded the blue and green horizontal lines in Figure 1E.

To compare the observed pattern of remapping with a null distribution that took into account the positions of the receptive fields and the stimulus probes, we recomputed the remapping vectors shown in Figure 1D after randomizing the relationship between the probe locations and the corresponding firing rates. Repeating this operation 100 times yielded a mean remapping vector that was significantly different from the observed one shown in Figure 1D, right (2 sample t-test, p < 0.001).

Supplemental References

S1. Neupane, S., Guitton, D., and Pack, C.C. (2016). Two distinct types of remapping in primate cortical area V4. Nature communications *7*, 10402.

S2. Zanos, T.P., Mineault, P.J., and Pack, C.C. (2011). Removal of spurious correlations between spikes and local field potentials. J Neurophysiol *105*, 474-486.

S3. Quiroga, R.Q., Nadasdy, Z., and Ben-Shaul, Y. (2004). Unsupervised spike detection and sorting with wavelets and superparamagnetic clustering. Neural Comput *16*, 1661-1687.

S4. Zirnsak, M., Steinmetz, N.A., Noudoost, B., Xu, K.Z., and Moore, T. (2014). Visual space is compressed in prefrontal cortex before eye movements. Nature *507*, 504-507.

Author contributions

S.N. designed the experiment, collected the data, analyzed the results, and wrote the paper. D.G. and C.C.P. designed the experiment and wrote the paper.